Computers and Mathematics with Applications 64 (2012) 877–886

Contents lists available at SciVerse ScienceDirect

Computers and Mathematics with Applications

journal homepage: www.elsevier.com/locate/camwa

Fuzzy incremental control algorithm of loop heat pipe cooling system for spacecraft applications

Su-Jun Dong, Yun-Ze Li *, Jin Wang, Jun Wang

School of Aeronautic Science and Engineering, Beihang University, Beijing 100191, China

ARTICLE INFO

Keywords:
Fuzzy incremental control
Loop heat pipe
Space cooling system
Modeling and simulation

ABSTRACT

Reliable and high precision thermal control technologies are essential for the safe flight of advanced spacecraft. A fuzzy incremental control strategy is proposed for control of an LHP space cooling system comprising a loop heat pipe and a variable emittance radiator with MEMS louver. The generating and performing algorithm of the fuzzy control rules is provided with an analytical form based on the understanding of dynamics and control mechanisms of the space cooling system. This paper also presents a novel integrated mathematical model for the dynamic analysis of the LHP space cooling system and a numerical evaluation of the investigated control schemes. Numerical simulation results on the closed loop control effects suggest that the proposed control strategy takes advantage of no steady error, small overshoots and short settling times; thus benefiting safe, highly accurate and reliable operation of the entire space cooling system. The overshoots of the most important operating parameters (T_{ob}, Q_r, and P) under the proposed fuzzy incremental control have been reduced to 16.3%, 17.6% and 18.6% of the compared PID control's, while the respective settling times have been shortened to 33.9%, 42.3% and 30.5% of the reference values.

1. Introduction

Loop heat pipes (LHPs), which have been experimentally investigated as an effective two-phase cooling technology for highly compacted electronic components like CPUs [1,2] with high power density in laptops and other ground systems, are considered to be a promising approach for the thermal control of the advanced space missions like robotic spacecraft [3], network missions on Mars [4], and nano-satellites [5]. The LHPs reduce flow resistance by separating the vapor line from the liquid line and the centralized capillary structure in the evaporator can pump the working fluid to a condensing placed more far away than the heat transfer distance of the traditional heat pipe, and it is also more convenient to form a central thermal collection network where multiple heat sources exist inside spacecraft [3–6]. Although LHPs are usually treated as a kind of passive thermal control method [6], the space cooling system which integrates LHP and variable emittance radiators like MEMS louver together can realize the high accurate active thermal control tasks by adjusting the heat radiation process at the outer surface of a space radiator [5,7–9]. However, this depends on a thorough understanding of the system dynamics and the considerate design of the active control schemes. A concise dynamic model and a practical control policy are required for the successful control of LHP space cooling systems.

Many efforts have been made to accomplish the modeling and simulation of the transient performances and the operating characteristics of LHPs. The steady-state heat transfer behaviors, the starting-up transients, and the temperature oscillations of 70 W miniature LHP were experimentally investigated in [10], and the transient heat and mass transfer processes in a

* Corresponding author. Tel.: +86 10 82338778.
E-mail addresses: dsj@buaa.edu.cn (S.-J. Dong), liyunze@buaa.edu.cn (Y.-Z. Li), wangjin05@ase.buaa.edu.cn (J. Wang), wangjun@buaa.edu.cn (J. Wang).

0898-1221/$ – see front matter © 2012 Elsevier Ltd. All rights reserved.
doi:10.1016/j.camwa.2012.01.030

cylindrical LHP evaporator were numerically investigated in [11]. A thermo-fluid dynamic model was proposed in [12] to determine the transient temperature distribution in the compensation chamber, the cavity and the condenser section of a stainless steel/ammonia LHP. Mathematic models, which predict the transient thermal behaviors of the space LHPs, have been developed and validated with ground-based experimental results in [13,14] independently. A more practical system level dynamical model has been developed in [15] and this model is suitable for numerical evaluation of the active control effects which are the focus in this paper.

Since the phase-change heat transfer mechanics inside LHPs and the heat dissipating processes at the outer surface at the variable emittance space radiators are all typical nonlinear processes, LHP space cooling systems are typical nonlinear controlled objects [16] which require robust, adaptive and practical control strategies like other nonlinear cooling, heating, and energy conversion processes in [17–19]. However little attention has been focused on the control technologies of the LHP space cooling system since LHPs are usually considered as passive thermal control approaches. The fuzzy logic methods [20,21] which were proved to be valid in the fields of spacecraft attitude control, signal integration and adaptive tracking control [22–26], were also reported as effective in resolving temperature control issues emerging in hydraulic heating [17], thermoelectric cooling [18], and energy conversion processes [19]. These reported fuzzy logic employed controllers include the adaptive fuzzy control scheme for the hydraulic heating process [17], the fuzzy coordinate control of TEC and its forced cooling fan in the nano-satellite space simulator [18]. These fuzzy control ideas are considered to be candidate solutions for the effective control of an LHP space cooling system for the controlled objects share similar nonlinear dynamic characteristics.

In the present research, a fuzzy incremental control strategy is developed with its rank associated generating and performing algorithm for linguistic fuzzy rules. This intelligent control strategy and algorithm take advantage of small overshoots, no steady error and robust operating properties. Moreover, they are much easier to perform using onboard computing devices of current spacecraft. Their closed loop control effects are numerically investigated and compared with that of a traditional PID control approach.

2. Fuzzy incremental control strategy and algorithm

As shown in Fig. 1(a), the controlled LHP space cooling system (LHP–SCS) comprises a loop heat pipe (LHP) and a variable emittance space radiator. The working fluid inside the LHP is ammonia, and the LHP consists of an evaporator, two transport lines for separate vapor and liquid flow, and a tube-type condenser attached to the inner side of the space radiator plate. As the exhaust heat is applied to the evaporator, it is transferred by conduction through the evaporator structure (in Fig. 1(b)) to vaporize the liquid inside. The vapor generated by the input heat travels along the vapor line to the condenser where heat is rejected to outer space by the variable emittance radiator and the vapor is condensed. The condensate enters the liquid line and is pumped back to the evaporator by the primary wick inside the evaporator which acts as a capillary pump and provides the major pressure head for the flowing working fluid. There is a small compensation chamber referred here as a reservoir inside the evaporator and a secondary wick provides the capillary path for fluid communication between the main part and the reservoir, as sketched in Fig. 1(b).

Fig. 1(c) illustrates the scheme of the variable emittance radiator. An MEMS louver array is mounted on the high emittance radiator surface to control the leaving heat flux. The cooling behavior of the radiator is dominated by the heat radiation between the spacecraft and its orbit environment since there is no air outside. When a louver cell in the MEMS array is opened, the high emittance radiator surface under it is exposed to the space environment; otherwise the low emittance surface of the cover cell will face space. Therefore, by controlling the number of open louver cells in the MEMS array, the whole cooling ability of the space cooling network can by be adjusted with ease. We define the exposing degree φ_r as the radiator surface ratio between the exposed area under the opened louver cells and the total area of radiator surface. The radiation heat flux leaving the radiator is governed approximately by (1).

$$Q_r = \varepsilon_e \sigma A T_r^4 = [(\varepsilon_h - \varepsilon_l)\,\varphi_r + \varepsilon_l]\,\sigma A T_r^4 \tag{1}$$

where σ is the Stefan–Boltzmann constant; A and T_r are total area and average temperature of the radiator surface; ε_e is the equivalent emittance of the radiator which can be determined by the emittance of the high emittance radiator surface (ε_h) and that of the MEMS louver cells (ε_l).

2.1. Principles and block diagrams of control strategies

The block diagrams of the controlled LHP–SCS and its fuzzy incremental controller (FIC) are illustrated in Fig. 2(a) and (b) respectively. The temperature of cooled object is measured and compared with its reference value, then the tracking error is fed to the FIC, as shown in Fig. 2(a). The FIC outputs the controlling variable which manipulates the exposing degree of the variable emittance radiator with the MEMS louver.

As shown in Fig. 2(b), the major parts of the FIC comprise a fuzzifier, an inference engine, a defuzzifier and a fuzzy rule base. Two auxiliary numerical operators are used for the real time differential and integral calculations of the error increment Δe_n and current controlling variable φ_r respectively. The control error e_n and its increment Δe_n are normalized by the factors K_e and K_c and then enter the fuzzifier; the produced linguistic values (E, CE) are compared with the fuzzy rules in the fuzzy

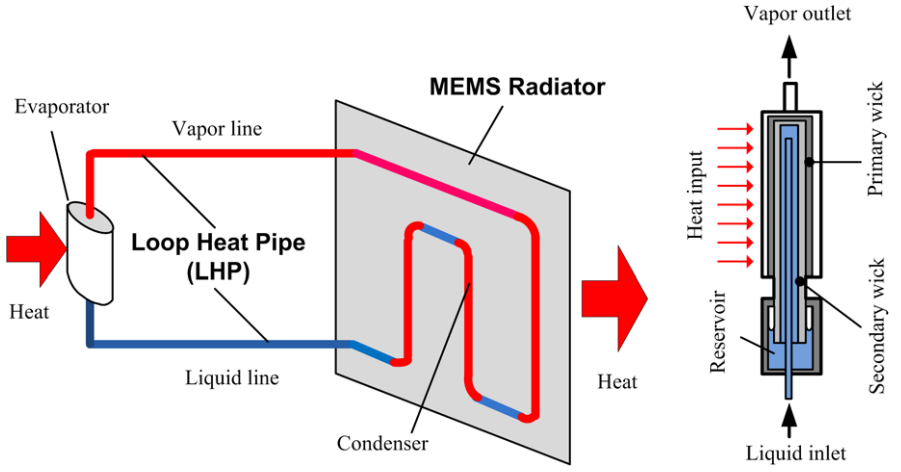

(a) LHP space cooling system.

(b) Evaporator of LHP.

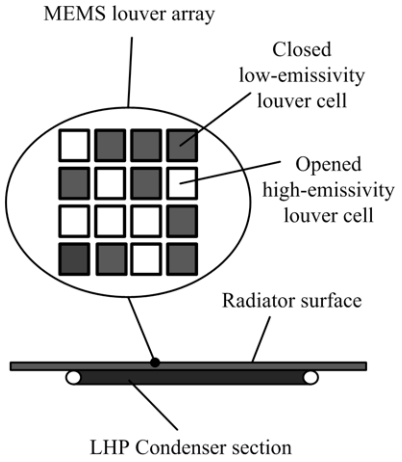

(c) Radiator with MEMS louver array.

Fig. 1. LHP space cooling system (LHP–SCS) and its components.

Table 1
Fuzzy sets and their linguistic value.

Fuzzy sets	Ranks	Linguistic values
NG	−4	Negative great
NL	−3	Negative large
NM	−2	Negative medium
NS	−1	Negative small
ZE	0	Zero
PG	4	Positive great
PL	3	Positive large
PM	2	Positive medium
PS	1	Positive small

rule base by the fuzzy inference engine. The fuzzy output is converted to a precise value at the defuzzifier. This output Δu_n represents the normalized increment of the controlling variable φ_r scaled by the factor K_u. The output of the FIC defuzzifier is fed to a digital integrator which has the function of memory. This FIC scheme takes advantage of easy construction, no static control error and reliable working ability. Therefore, it is very suitable for spacecraft applications.

2.2. Control rules and their performing algorithms

A nine-element fuzzy set system {NG, NL, NM, NS, ZE, PS, PM, PL, PG} in Table 1 is used to characterize the linguistic values of e_n, Δe_n and Δu_n. Each fuzzy set (or its linguistic value) is associated with a crisp number as an analytical rank for

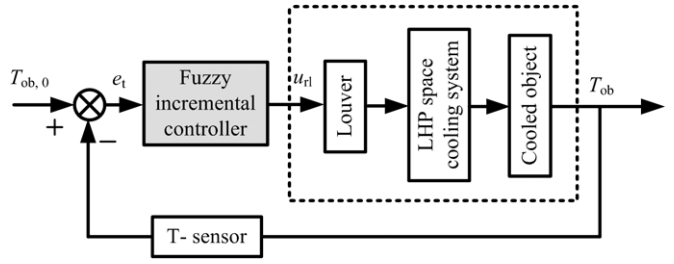

(a) Fuzzy incremental control system context.

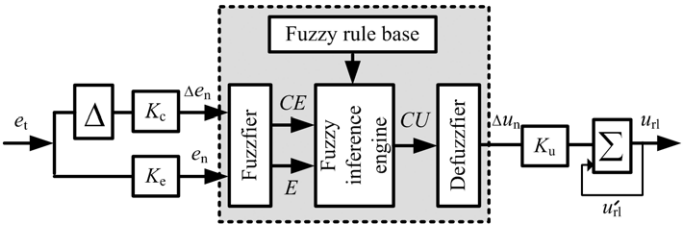

(b) Implementation of fuzzy incremental controller.

Fig. 2. Block diagram of the fuzzy incremental control scheme.

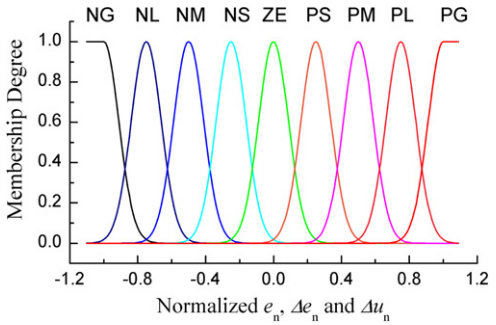

Fig. 3. Membership functions of the fuzzy sets.

the convenient performance of the control rules. As shown in Fig. 3, the membership functions, $\mu(x, k)$, of the above fuzzy sets are determined by the following Gaussian equation.

$$\mu(x, k) = \exp\left(\frac{x - (k \times a)}{b}\right)^2 \tag{2}$$

where $x \in \{e_n, \Delta e_n, \Delta u_n\}$, k is the analytical rank associated with the focused fuzzy set in Table 1, a is set to 0.25, the value of b which can be regulated when necessary, is set to 0.125 here. When x exceeds the range $(-1, 1)$, the membership degrees of boundary fuzzy sets (NG and PG) are given by (3):

$$\begin{aligned} &\mu(x, -4) = 1, \quad x < -1 \\ &\mu(x, 4) = 1, \quad x > 1. \end{aligned} \tag{3}$$

The linguistic control rules of FIC can be constructed using the following general form:

$$\text{IF } e_n \text{ is } E_i \text{ and } \Delta e_n \text{ is } CE_j, \text{ THEN } \Delta u_n \text{ is } CU_{\ell(i,j)} \tag{4}$$

where E_i and CE_j and $CU_{\ell(i,j)}$ are the fuzzy values of e_n, Δe_n and Δu_n; the subscript variables i, j and $\ell(i, j)$ denote the analytical ranks associated with these linguistic values in Table 1.

Theoretical analysis and simulation study of the LHP space cooling system dynamics suggest that a suitable control action at different control situations should be in accord with the following fundamentals:

(1) A positive e_n usually requires a negative controlling variable increment when Δe_n is very small, and a negative e_n often requires a positive one under the same situation.
(2) A large e_n needs a large controlling variable increment while a small Δu_n is suitable for small e_n, whether e_n is positive or negative.

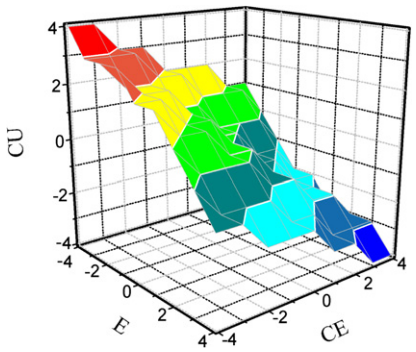

Fig. 4. Surface map of the fuzzy incremental control rules.

(3) A positive Δe_n will strengthen the requirement for a negative controlling variable increment when e_n is positive and alleviate the positive controlling variable increment value when e_n is negative.
(4) Similarly, a negative Δe_n will strengthen the positive incremental trend of the controlling variable when e_n is negative and alleviate the negative intention of the controlling variable increment when e_n is positive.
(5) When the absolute value of e_n is small, the impact of the control error change Δe_n should be large, otherwise the impact should be small.

On the basis of these control knowledge insights, a rank-based generating and performing algorithm for the fuzzy rules in (4) is derived in

$$\ell(i, j) = -1 \times \text{nInt}\left(\omega_i \times i + (1 - \omega_i) \times j\right) \tag{5}$$

where ω_i is the error impact power determined by the rank of the input error ($\omega_i = 0.4$ for $i = 0, 1$, $\omega_i = 0.5$ for $i = 2$ and $\omega_i = 0.6$ for $i = 3, 4$); the return value of the function nInt (x) is the nearest integer number of the input x.

Fuzzy control rules which are produced by (5) for the intelligent control of the LHP space cooling system are plotted in Fig. 4.

If all the fuzzy control rules from (5) are treated equally, the output of the defuzzifier in Fig. 2(b) can be calculated by

$$\Delta u_n = \sum_{i=1}^{9}\sum_{j=1}^{9} u_{\text{rnc},\ell(i,j)}\lambda_{\ell(i,j)} \Big/ \sum_{i=1}^{9}\sum_{j=1}^{9} \lambda_{\ell(i,j)} \tag{6}$$

where $u_{\text{rnc},\ell(i,j)}$ and $\lambda_{\ell(i,j)}$ are the representative value and membership degree of the output fuzzy set $CU_{\ell(i,j)}$ for the $i\times 9+j$th control rule, and they are determined by (7) and (8), respectively.

$$u_{\text{rnc},\ell(i,j)} = \ell(i, j) \times a \tag{7}$$

$$\lambda_{l(i,j)} = \text{Min}[\mu(e_n, i), \mu(\Delta e_n, j)]. \tag{8}$$

Otherwise, the output-decision membership of the outputs which belong to CU_k, $(k = -4, -3, \ldots, +3, +4)$ takes the form of

$$\mu_{f,k} = \sum_{i=1}^{9}\sum_{j=1}^{9} \min\left\{\mu(e_n, i), \mu(\Delta e_n, j), \mu_{r,i\times 9+j}\right\} | \ell(i, j) = k \tag{9}$$

where $\mu_{r,i\times 9+j}$ is the power of the $i \times 9 + j$th control rule from (5).

And the output of the defuzzifier becomes

$$\Delta u_n = \sum_{k=-4}^{4} u_{\text{rnc},k}\mu_{f,k} \Big/ \sum_{k=-4}^{4} \mu_{f,k} \tag{10}$$

where $u_{\text{rnc},k}$ the representative values of fuzzy set CU_k.

Finally, after the above T–S alike fuzzy inference mechanisms, the controlling variable φ_r is determined in terms of the normalize incremental of Δu_n and the controlling variable value φ_r' at previous sampling time by

$$\varphi_r = \varphi_r' + K_u \Delta u_n \tag{11}$$

where K_u is scale factor of the controlling variable.

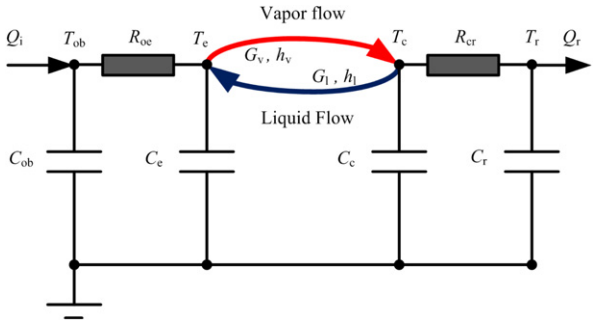

Fig. 5. 4-nodal thermal network model of LHP–SCS.

Table 2
The elements of the system matrix R_{sys}.

Elements	Expressions
r_1	$1/R_{oe}$
r_2	$(C_c/C_{hp})\,(1/R_{oc})$
r_3	$(1-C_c/C_{hp})\,(1/R_{cr})$
r_4	$1/R_{oc}$
r_5	$1/R_{cr}$

3. Simulation validation of the control effects

3.1. Mathematical model of the controlled LHP–SCS

The dynamics of LHP–SCS can be effectively determined by 4-nodal thermal networks which are shown in Fig. 5. In this thermal network model, the LHP–SCS is treated as four lumped parameter nodes which include the cooled object and (T_{ob} with the thermal capacity of C_{ob}), the radiator (T_r with the thermal capacity of C_r), the LHP evaporator (T_e with the thermal capacity of C_e) and the LHP condenser (T_c with the thermal capacity of C_c); thus the transient temperatures of the entire space cooling system can be expressed by the following differential equation group (more detailed information is provided by [15]).

$$\mathbf{C_{sys}}\begin{bmatrix}\dot{T}_{ob}\\ \dot{T}_e\\ \dot{T}_c\\ \dot{T}_r\end{bmatrix}=\mathbf{R_{sys}}\begin{bmatrix}T_{ob}\\ T_e\\ T_c\\ T_r\end{bmatrix}+\begin{bmatrix}Q_i\\ 0\\ 0\\ Q_{ex}-[(\varepsilon_h-\varepsilon_l)\,\varphi_r+\varepsilon_l]\,\sigma A_r T_r^4\end{bmatrix} \tag{12}$$

where Q_i and Q_{ex} are the exhaust heat of the cooled object and the total external heat load radiated from the sun and the earth.

$\mathbf{C_{sys}}$ is the thermal capacity distribution matrix which is determined by

$$\mathbf{C_{sys}}=\mathrm{Diag}[C_{ob}\quad C_e\quad C_{hp}\quad C_r] \tag{13}$$

where C_{hp} is the thermal capacity of the entire LHP.

$\mathbf{R_{sys}}$ is the thermal resistance matrix which can be expressed as

$$\mathbf{R_{sys}}=\begin{bmatrix}-r_1 & r_1 & 0 & 0\\ r_1-r_2 & -r_1 & r_2-r_3 & r_3\\ r_4 & 0 & -r_4-r_5 & r_5\\ 0 & 0 & r_5 & -r_5\end{bmatrix} \tag{14}$$

where r_i $(0<i<6)$ are the matrix elements which are determined by Table 2.

In the above equations, R_{oe} is thermal resistance between the cooled object and the evaporator, R_{oc} and R_{cr} are the thermal resistances between the cooled object, the LHP condenser section and the radiator.

Then according to the conclusions of [15], the working fluid mass flow rate G_{hp} inside LHP can be approximately calculated from the nodal temperatures by

$$G_{hp}=\frac{1}{h_v-h_l}\left\{\frac{C_c}{C_{hp}}\frac{(T_{ob}-T_c)}{R_{oc}}+\left(1-\frac{C_c}{C_{hp}}\right)\frac{(T_c-T_r)}{R_{cr}}\right\} \tag{15}$$

where h_v and h_l are the respective specific enthalpies of the vapor and the liquid.

Table 3
Parameters of the working fluid pressure equation.

Parameters	Values
A_0	4.293025E−1
A_1	1.605853E−2
A_2	2.351689E−4
A_3	1.558870E−6
A_4	2.940981E−9
A_5	1.322185E−12

Table 4
Parameters of simulated controllers.

Sampling period, $T_s = 1.0$ s	
Parameters	Values
Fuzzy incremental controller	
K_e	0.0083
K_c	0.526
K_u	0.12
PID controller	
K_p	−2.1
T_i	162.0
T_d	0.001

Table 5
Parameters of the controlled LHP space cooling system.

Parameter (Unit)	Symbol	Value
Design working parameters		
Cooling ability (W)	Q_i	50
Cooled object temperature (K)	T_{ob}	371.65
Radiator temperature (K)	T_r	308.15
Heat pipe condensing temperature (K)	T_c	314.15
System characteristic parameters		
Thermal capacity of cooled object (J/K)	C_{ob}	45.2
Thermal capacity of radiator (J/K)	C_r	135.6
Thermal resistance of heat pipe (K/W)	R_{hp}	1.0
Thermal resistance between cooled object and heat pipe (K/W)	R_{oe}	0.15
Thermal resistance between heat pipe and radiator (K/W)	R_{cr}	0.12

Using the condenser temperature as the representative temperature of the working fluid, the condensing pressure inside the heat pipe is given by (13).

$$P = A_0 + \sum_{i=1}^{5} A_i (T_c - 273.15)^i \tag{16}$$

where P the condensing pressure of the working fluid. The calculating parameters A_i for the employed ammonia are fitted and listed in Table 3.

3.2. Simulation case and system parameters

To validate the control effects of the proposed FIC, we numerically investigated an LHP–SCS which was controlled by the proposed FIC and another traditional PID controller for comparison. Tables 4 and 5 give the parameters of the simulated controllers and controlled LHP space cooling system respectively, and a typical −10% step change in the system cooling load Q_i is computed and discussed in detail as an example.

3.3. Discussions on the numerical results

The numerical results on temperature, heat flux, and controlling variable responses of the cooled object and the space radiator are depicted in Figs. 6 and 7. The thermal and hydraulic transients of LHP temperatures, condensing pressure and mass flow rate are plotted in Figs. 8 and 9. The values of the settling time and overshoot for the above transients are calculated in Table 6 for the purpose of quantitative evaluation of the control effects.

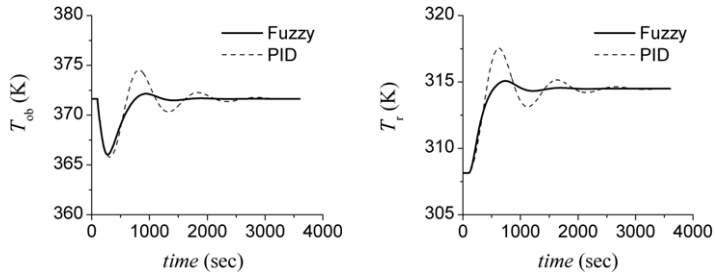

(a) Cooled object. (b) Radiator.

Fig. 6. Temperature control effects on cooled object and radiator.

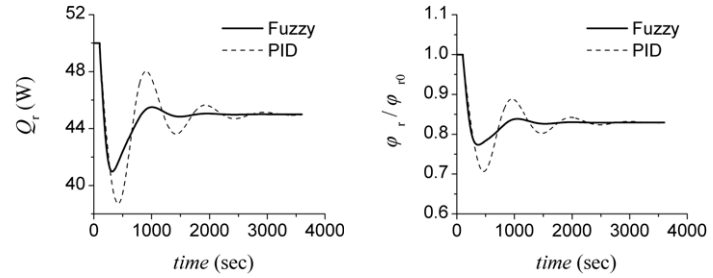

(a) Radiated heat. (b) Exposing degree.

Fig. 7. Heat flux tracking effects and the exposing degree responses.

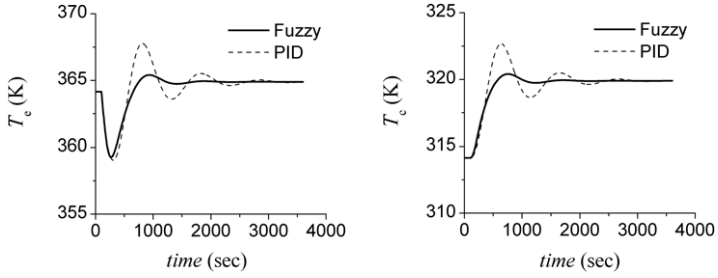

(a) LHP evaporator. (b) LHP condenser.

Fig. 8. Controlled LHP temperature responses.

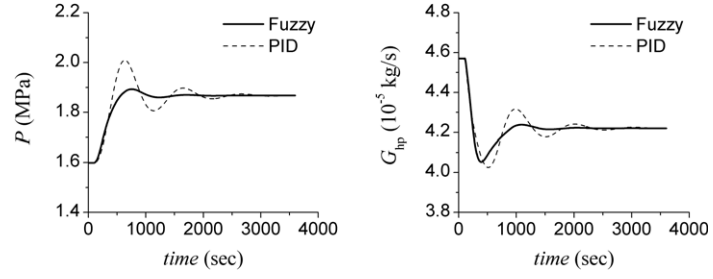

(a) Condensing pressure. (b) Mass flow rate.

Fig. 9. Controlled LHP hydraulic responses.

Observations and discussions on the numerical simulation results are concluded and summarized as follows:

(1) *Temperature control and heat flux tracking effects* (Figs. 6 and 7, Table 6)

The temperature control and heat flux tracking effects of our proposed FIC are superior than that of the compared PID scheme for smaller settling times and smaller overshoots.

Table 6
Comparisons on close loop settling times and overshoots.

	PID		FIC (Fuzzy)		Comparisons	
	τ/s[a]	σ/unit[b]	τ/s	σ/unit	τ_{FIC}/τ_{PID}	$\sigma_{FIC}/\sigma_{PID}$
T_{ob}	1825	2.83	620	0.46	0.339	0.163
T_r	1619	3.03	724	0.57	0.447	0.189
T_e	1833	2.92	924	0.6	0.504	0.209
T_c	1627	2.69	402	0.49	0.247	0.182
Q_r	1458	6.8	617	1.2	0.423	0.176
φ_r/φ_{r0}	1573	−15.1	619	−6.6	0.394	0.437
P	1195	7.0	366	1.3	0.305	0.186
G_{hp}	986	−4.7	532	−4.0	0.539	0.851

[a] The error bands are 0.5 K for temperatures, and 2% final value for others.
[b] The overshoot unit are 'K' for temperatures, '%' for others.

- The cooled object temperature (T_{ob}, in Fig. 6(a)) is well controlled at its reference value. The settling time and overshoot are only 33.9% and 16.3% of the corresponding values of the compared PID control. Similar improvements are observed with the radiator temperature (T_r, in Fig. 6(b)) which is not selected as a controlled variable.
- The cooling heat flux of radiator (Q_r, in Fig. 7(a)) matches the input cooling load change more quickly and accurately than what PID does, the corresponding values of settling time and overshoot are reduced to 42.3% and 17.6% respectively.
- As the only controlling variable, the exposing degree of the radiator (φ_r, in Fig. 7(b)) responds more smoothly and therefore more effectively under the proposed FIC, the settling time is shortened to 39.4% while the overshoot is reduced to 43.7%, and this means the actors under FIC can working more efficient and reliably than under the compared PID.

(2) *Thermal and hydraulic operating parameters of LHP* (Figs. 8 and 9, Table 6)

The proposed FIC provides a more stable and more safe thermal/hydraulic operating condition for LHP structure and working fluid than the PID does.

- The temperature fluctuation has been successfully controlled (T_e and T_c, in Fig. 8). The T_e waving amplitude is only 20.9% of that under PID, and the waving process has been shortened to 50% according to the overshoots and settling times in Table 6. The respective values for T_c are 18.2% and 24.7%.
- For the condensing pressure (P, in Fig. 9(a)) which is most important fact for the LHP safety operating in the space vacuum environment, the oscillation amplitude and lasting time are reduced to 18.6% and 13.5% compared to that under PID control.
- The settling time of the working fluid flow rate change (G_{hp}, in Fig. 9(a)) is shortened to 53.9% of that under PID while the overshoot is reduced to 85.1%. These will benefit the hydraulic operating condition of LHP.

4. Conclusions

A Fuzzy Incremental Control strategy was proposed for the effective and reliable control of an LHP space cooling system. The control effects of the proposed FIC were numerically investigated. The numerical analysis on the control effects suggest that the overshoots and settling times of the controlled variable and the operating state parameters of the controlled LHP space cooling system have been obviously reduced under the proposed FIC scheme compared with the traditional PID approach. For the most important parameters (T_{ob}, Q_r, and P), the respective overshoots have been reduced to 16.3%, 17.6% and 18.6%, while the settling times are 33.9%, 42.3% and 30.5% respectively. These mean that the proposed FIC not only improves the temperature control and heat flux tracking effect obviously, but also promises a more stable thermal and hydraulic conditions for the safe operating of the LHP structures and working fluid. The control strategy and numerical investigation results in this research are expected to benefit the thermal control system design of advanced spacecraft where LHP cooling systems are employed. These potential missions include nano-satellites, space robots, lunar rovers and Mars landers.

Acknowledgment

This work was supported by National Natural Science Foundation of China under Grant 50506003.

References

[1] Y.F. Maydanik, S.V. Vershinin, M.A. Korukov, J.M. Ochterbeck, Miniature loop heat pipes a promising means for cooling electronics, IEEE Transactions on Components and Packaging Technologies 28 (2005) 290–296.
[2] R. Singh, A. Akbarzadeh, C. Dixon, M. Mochizuki, R.R. Riehl, Miniature loop heat pipe with flat evaporator for cooling computer CPU, IEEE Transactions on Components and Packaging Technologies 30 (2007) 42–49.
[3] T.D. Swanson, G.C. Biru, NASA thermal control technologies for robotic spacecraft, Applied Thermal Engineering 23 (2003) 1055–1065.
[4] R. Nadalini, F. Bodendieck, The thermal control system for a network mission on Mars: the experience of the Netlander mission, Acta Astronautica 58 (2006) 564–575.

[5] G. Birur, Advanced thermal control architecture for future spacecraft, in: Presented at the 12th Annual Spacecraft Thermal Control Technology Workshop, El Segundo, California, February 28, 2001.
[6] R.R. Riehl, T. Dutra, Development of an experimental loop heat pipe for application in future space missions, Applied Thermal Engineering 25 (2005) 101–112.
[7] D.M. Douglas, J. Ku, L. Ottenstein, T. Swanson, S. Hess, A. Darrin, Effect of variable emittance coatings on the operation of a miniature loop heat pipe, in: AIP Conference Proceedings, vol. 746, 2005, pp. 82–89.
[8] R. Osiander, S.L. Firebaugh, J.L. Champion, D. Farrar, M.A.G. Darrin, Microelectromechanical devices for satellite thermal control, IEEE Sensors Journal 4 (2004) 525–531.
[9] D. Farrar, W. Schneider, R. Osiander, J.L. Champion, A.G. Darrin, D. Douglas, et al. Controlling variable emittance (MEMS) coatings for space applications, in: 8th Intersociety Conf. on Thermal and Thermomechanical Phenomena in Electronic Systems, 2002, pp. 1020–1024.
[10] Y. Chen, M. Groll, R. Mertz, Y.F. Maydanik, S.V. Vershinin, Steady-state and transient performance of a miniature loop heat pipe, International Journal of Thermal Sciences 45 (2006) 1084–1090.
[11] K.N. Shukla, Thermo-fluid dynamics of loop heat pipe operation, International Communications in Heat and Mass Transfer 35 (2008) 916–920.
[12] M.A. Chernysheva, Yu.F. Maydanik, Numerical simulation of transient heat and mass transfer in a cylindrical evaporator of a loop heat pipe, International Journal of Heat and Mass Transfer 51 (2008) 4204–4215.
[13] V.V. Vlassov, R.R. Riehl, Mathematical model of a loop heat pipe with cylindrical evaporator and integrated reservoir, Applied Thermal Engineering 28 (2008) 942–954.
[14] T. Kaya, R. Pérez, C. Gregori, A. Torres, Numerical simulation of transient operation of loop heat pipes, Applied Thermal Engineering 28 (2008) 967–974.
[15] Y.-Z. Li, Y.-Y. Wang, K.-M. Lee, Dynamic modeling and transient performance analysis of a LHP–MEMS thermal management system for spacecraft electronics, IEEE Transactions on Components and Packaging Technologies 33 (2010) 597–606.
[16] W. Shi, M. Zhang, W. Guo, L. Guo, Stable adaptive fuzzy control for MIMO nonlinear systems, Computers & Mathematics with Applications 62 (2011) 2843–2853.
[17] C. Haissig, Adaptive fuzzy temperature control for hydraulic heating systems, IEEE Control Systems Magazine 20 (2000) 39–48.
[18] Y.-Z. Li, K.-M. Lee, J. Wang, Analysis and control of equivalent physical simulator for nanosatellite space radiator, IEEE/ASME Transactions on Mechatronics 15 (2010) 79–87.
[19] D. Matko, I. Škrjanc, G. Mušič, Robustness of fuzzy control and its application to a thermal plant, Mathematics and Computers in Simulation 51 (2000) 245–255.
[20] Y. Zhao, Y. Zhu, Fuzzy optimal control of linear quadratic models, Computers & Mathematics with Applications 60 (2010) 67–73.
[21] C.-L. Chen, P.-C. Chen, C.-K. Chen, Analysis and design of fuzzy control system, Fuzzy Sets and Systems 57 (1993) 125–140.
[22] C.-H. Cheng, S.-L. Shu, Application of fuzzy controllers for spacecraft attitude control, IEEE Transactions on Aerospace and Electronic Systems 45 (2009) 761–765.
[23] G.-S. Huang, H.-J. Uang, Robust adaptive PID tracking control design for uncertain spacecraft systems: a fuzzy approach, IEEE Transactions on Aerospace and Electronic Systems 42 (2006) 1506–1514.
[24] C.-L. Chen, C.-L. Tai, Adaptive fuzzy color segmentation with neural network for road detections, Engineering Applications of Artificial Intelligence 23 (2010) 400–410.
[25] Y.-Y. Lin, M.-Y. Liao, Image processor and fuzzy PID controller design for robot-car intercept mission, Journal of the Chinese Society of Mechanical Engineers 30 (2009) 401–408.
[26] Her-Terng Yau, Chieh-Li Chen, Chattering-free fuzzy sliding-mode control strategy for uncertain chaotic systems, Chaos, Solitons & Fractals 30 (2006) 709–718.